AIP Conference Proceedings

Performance characterization of a wells turbine under unsteady flow conditions

Cite as: AIP Conference Proceedings **2191**, 020149 (2019); https://doi.org/10.1063/1.5138882
Published Online: 17 December 2019

Marco Torresi, Michele Stefanizzi, Francesco Fornarelli, Luana Gurnari, Pasquale Giuseppe Fabio Filianoti, and Sergio Mario Camporeale

View Online Export Citation

ARTICLES YOU MAY BE INTERESTED IN

Vertical axis air turbine in oscillating water column systems
AIP Conference Proceedings **2191**, 020027 (2019); https://doi.org/10.1063/1.5138760

Pump as turbine for throttling energy recovery in water distribution networks
AIP Conference Proceedings **2191**, 020142 (2019); https://doi.org/10.1063/1.5138875

AIP Publishing

© 2019 Author(s).

Performance characterization of a Wells turbine under unsteady flow conditions

Marco Torresi[1, a)], Michele Stefanizzi[1)], Francesco Fornarelli[1)], Luana Gurnari [2)], Pasquale Giuseppe Fabio Filianoti[2)], Sergio Mario Camporeale[1)]

[1]*Department of Mechanics, Mathematics and Management, Polytechnic University of Bari, 70125 Bari, Italy*
[2]*Department of Civil, Energy, Environment and Materials Engineering, Mediterranean University of Reggio Calabria, 89124 Reggio Calabria, Italy*

[a)]Corresponding author: marco.torresi@poliba.it

Abstract. In the open wind tunnel of the Polytechnic University of Bari a new 3D-printed prototype of a Wells turbine is investigated under steady-state and pulsating flow conditions. The flow rate is modified by changing sinusoidally the frequency of the control drive, hence the rotational speed of the suction fan. The Wells turbine is a scaled prototype designed to operate in a 1:10 scaled model of a REWEC3 breakwater for ocean application. The Wells turbine characteristics are evaluated in terms of torque coefficient and pressure drop coefficient vs. flow coefficient. A delayed onset of stall can be observed, with a clockwise hysteretic loop, when the turbine experiences large sinusoidal variation of the flow coefficient at high mass flow rates. The variation of the turbine performance under dynamic flow conditions is crucial for a correct design of the Wells turbine.

INTRODUCTION

According to the latest report by the International Renewable Energy Agency (IRENA) [1], despite the clear evidence of human-caused climate changes, the Nations' commitments under the Paris Agreement on climate change and the increase of sustainable energy productions, energy-related carbon dioxide (CO_2) emissions have increased 1.3% annually, on average, over the last five years. The gap between observed emissions and the reductions that are needed to meet internationally agreed climate objectives is widening. For this reason, in recent years energy and environmental policies are increasingly encouraging the development of clean and renewable energy sources.

Two thirds of the earth surface are covered by oceans and seas, which can be fundamental renewable sources. Despite of resources such as the sun and the wind, which show a consolidated and confirmed potential, the scientific community is making a consistent effort in finding innovative solutions to produce clean energy from marine energy (and particularly wave energy) with no environmental impact. Obviously, not all sites are suitable for marine energy harvesting either for the water characteristics (e.g., presence of sediments) or for the impact of these installations on those coasts with a strong tourist vocation [2]. In the first case, a monitoring of the sea water quality (for instance, by means of measurement systems such as GeoLab [3]) can help in the site selection procedure. The global gross theoretical wave resource can be evaluated (based on data from a global wind-wave model and buoy data) in 3.7 TW; whereas the global net power resource (excluding both areas where the power is lower than 5 kW/m and potentially ice-covered areas) can be estimated equal to 3.0 TW [4].

The difficulty that is found in the use of this technology is due to the unpredictability of extreme events that can lead to irreversible damage to coastal structures and the devices they contain. The predisposition to the exploitation of the wave motion varies therefore from country to country and strongly depends on the temporal variability of the energy available from the wave motion.

Indeed, Cornett [5] states that sites characterized by more stable and moderate waves are more preferable than very energetic sites that do not boast a constant wave regime. Lopez [6], confirms this theory by adding that an

74th ATI National Congress
AIP Conf. Proc. 2191, 020149-1–020149-9; https://doi.org/10.1063/1.5138882
Published by AIP Publishing. 978-0-7354-1938-4/$30.00

unexpected high energy availability would cause damage to the energy conversion system and furthermore this would not allow to work in conditions of maximum efficiency for stable ranges of period and wave height.

The typical first generation of Wave Energy Converters (WEC) is the Oscillating Water Column (OWC) device, depicted in Fig. 1. The oscillatory movement of the water contained in an appropriately designed chamber alternately determines the phases of compression and expansion of the air overlying, which is forced to cross in both directions a duct, where a turbine is installed. Since the air flow direction and its speed are oscillating, it is necessary to install a turbine that maintains the same direction of rotation even if the flow reverses its direction.

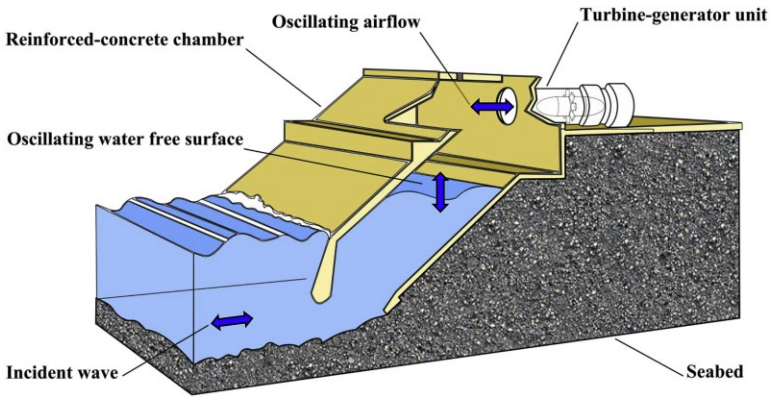

FIGURE 1. Schematic of an OWC device (adapted by Hashem et al. [7]).

Usually, Wells turbines represent the most common solution to convert the energy of this oscillating air flow into work [8]. The advantages of this technology are the architectural simplicity and its reliability; however, one of its major drawbacks are commonly related to the limited operating range due to blade stall at high flow rate [9]. The combined system constituted by the OWC device and the Wells turbine, behaves as a mechanic mass-spring-damper system. The turbine contributes to the damping factor. This means that, in order to maximize the annual energy output, the turbine characteristics must be optimized.

In this framework, a Wells turbine has been designed and manufactured by means of a 3-D printer. Then the machine has been tested at the GaVe-PrInCE laboratory of the Polytechnic University of Bari in order to investigate its performance both in steady-state and unsteady flow conditions.

THE WELLS TURBINE

The Wells turbine is a low-pressure air turbine that rotates continuously in the same direction regardless the direction of the air flow. Its blades are characterized by symmetrical airfoils staggered at a 90 degrees angle. Fig. 2 illustrates the forces acting on the blades of Wells turbines.

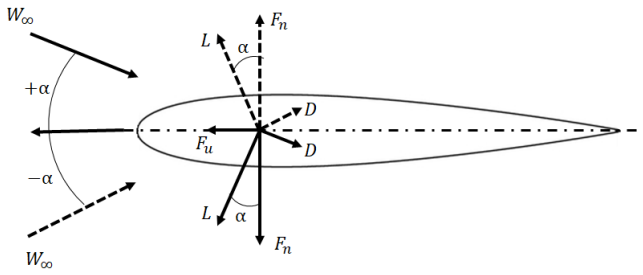

FIGURE 2. Forces acting on the Wells turbine blade.

Given an axial velocity, V, and a tangential rotor velocity U, the relative flow velocity, W_∞, creates an angle, α, with respect to the blade chord. Hence, a lift, L, and a drag, D, are generated, perpendicular and parallel to W_∞, respectively. These forces can be resolved into the tangential, F_u, and the axial, F_n, forces, whose magnitude varies during the cycle. However, the F_u direction is predominantly independent of the flow direction. F_u will be negative

whenever the drag becomes dominant, namely, either when the flow rate approaches zero or when stall conditions occur [10]. Another important feature of the Wells turbine is related to its high rotational speed, which allows the direct coupling with electrical generators and a significant energy storage by the fly-wheel effect simplifying the constant speed control [11].

Figure 3 shows the new small-scale Wells turbine under investigation. The turbine design (i.e. the definition of the turbine solidity, hub to tip ratio, and the blade airfoil) has been carried out in order to be able to match the Wells turbine with a REWEC (Resonant Wave Energy Converter) breakwater, which is was located off the beach of Reggio Calabria, Italy. The components of the turbine rotor have been manufactured by means of a 3-D printer (Stratasys Object30 Pro) by using the VeroClear material, a transparent PolyJet photopolymer. The main specifications of the 3-D printer are the layer thickness equal to 16 μm and the typical deviation from STL dimensions of ±100 μm. The main geometric parameters of the rotor are summarized in table 1. The blades, technically drawn in figure 4, are characterized by constant chord a NACA0015 blade profile.

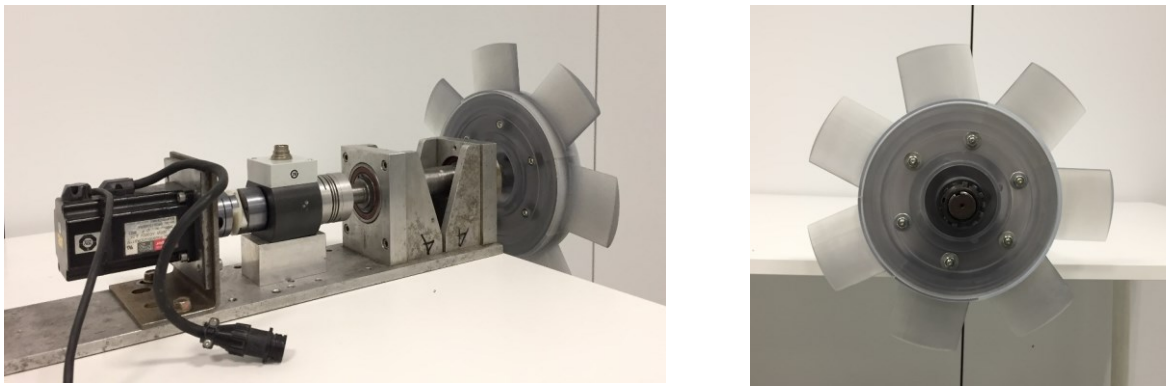

(a) (b)

FIGURE 3. The small-scale model of the Wells turbine off the air tube (a); Assembly view of the turbine (b).

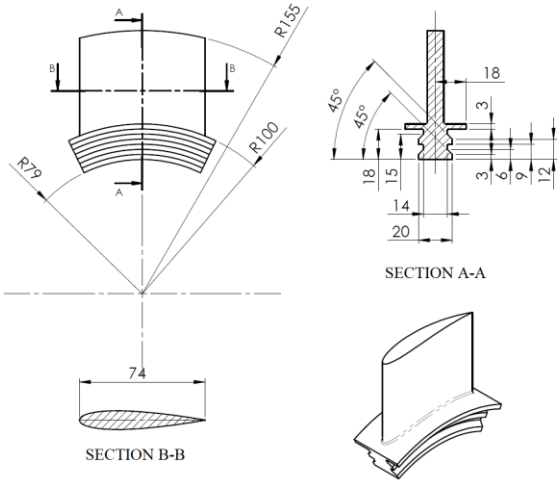

FIGURE 4. Detailed drawing of the small-scale Wells turbine.

TABLE 1. Main geometric parameters of the turbine under investigation.

R_{hub} [mm]	R_{tip} [mm]	Blade chord c [mm]	Number of blades
100	155	74	7

The performance of the Wells turbine is provided in terms of non-dimensional parameters, namely the torque coefficient, T^*, the stagnation pressure drop coefficient, Δp^*, the flow coefficient U^* and the efficiency, η. The torque coefficient, T^*, is defined as follows:

$$T^* = \frac{T_t}{\rho_a \, \omega^2 \, R_{tip}^5} \tag{1}$$

where T_t is the Wells turbine torque, ρ_a is the air density, ω is the angular speed, R_{tip} is the blade tip radius.

The stagnation pressure drop coefficient, Δp^*, is defined as follows:

$$\Delta p^* = \frac{\Delta p_0}{\rho_a \, \omega^2 \, R_{tip}^2} \tag{2}$$

where Δp_0 is the stagnation pressure drop across the turbine.

The flow coefficient U^* is defined as follows:

$$U^* = \frac{V}{\omega R_{tip}} \tag{3}$$

where V is the average axial velocity in the annular section upstream the turbine, computed from the volumetric flow rate, Q, and the annulus area, A_t, as follows:

$$V = \frac{Q}{A_t} \tag{4}$$

The pneumatic power, P_p, generated by the air flow rate, Q, is related to the pressure drop, Δp_0, across the turbine

$$P_p = Q \Delta p_0 \tag{5}$$

Finally, the turbine efficiency, η, can be evaluated as follows:

$$\eta = (T_t \omega)/P_p \tag{6}$$

THE TEST RIG

The experimental campaign has been carried out at the GaVe laboratory of the Polytechnic University of Bari. Figure 5 shows the test rig, which is basically a low-speed, open circuit wind tunnel of the suction type.

The first part of the wind tunnel is constituted by a convergent duct (1m long) with an inlet diameter equal to 455 mm and an outlet diameter equal to 314 mm. The dimensions of the settling chamber are 1.5m × 1.0m × 1.0m (L × W × H). The chamber is divided into two parts by a honeycomb in order to straighten the flow because swirling winds in the tunnel appear.

A squirrel cage blower (model A0 112M – 4 by ELPROM) is installed in the final part of the wind tunnel with the aim to generate the air stream through the Wells turbine. An AC electric motor (2 poles, nominal power equal to 4.1 kW at 1430 rpm) drives the fan. A compact vector control drive, model V1000 by Omron (nominal power of 5.5 kW) adjusts the voltage and frequency to power the AC motor.

The flow measurements are performed on the pipe which connects the blower to the settling chamber. Indeed, the flow rate measurement is performed according to the ISO 5147-1 standard, by means of orifice plates chosen as pressure differential devices. Orifices of different diameter ratio, β, have been considered (namely 0.2, 0.3, 0.4, 0.5, 0.6 and 0.75) in order to reduce measurement uncertainty at the different flow rates.

FIGURE 5. View of the test rig used for the experimental campaign of the small-scale Wells turbine.

The relative pressure upstream of the orifice is measured by means of a Honeywell 163PC01D36 amplified pressure transducer. This is characterized by a pressure range of ±5″H_2O, a combined Null and Sensitivity Shift ±1%span, repeatability and hysteresis ±0.25 %span. The differential pressure value across the orifice is measured by means of a Honeywell 164PC01D76 amplified pressure transducer. This device is characterized by a pressure range of 0÷5″H_2O, a combined Null and Sensitivity Shift ±1.25%span, repeatability and hysteresis ±0.25 %span.

The Wells turbine under investigation is connected to a P-Series SanyoDenky Servo Motor used as electric generator. An HBM T22/5NM torque meter is installed to measure the turbine torque (±0.5%span sensitivity tolerance).

The stagnation pressure drop across the Wells turbine is measured by means of a second Honeywell 163PC01D36 amplified pressure transducer. Actually, the pressure difference is evaluated connecting the transducer on one side at a pressure tap in the settling chamber and leaving the other side open to the atmosphere, neglecting the minor pressure losses at the air duct ends and at the turbine hub.

The entire test bench is managed by means of a Supervisor Control and Data Acquisition (SCADA) developed in the NI LabVIEW® environment.

Since the evaluation of the mass flow rate, according to the ISO 5147-1 standard, requires an iterative procedure, the final results are elaborated by means of a code written in MATLAB.

EXPERIMENTAL CHARACTERIZATION

The Wells turbine has been tested at a constant rotational speed, n = 1750 rpm, both under steady state and pulsating flow conditions. The experimental characterization has been carried out for a wide range of flow rates by varying the rotational speed of the wind tunnel blower. During the steady state tests, actually, the blower rotational speed has been changed by increasing the output frequency of the V1000 Omron's vector control drive from 5 Hz up to 60 Hz with steps equal to 5 Hz. Moreover, orifices with different diameter ratio, β, have been settled in order to guarantee the maximum accuracy and the lower uncertainty, while limiting the pressure losses across the orifice, at each flow rate.

Figures 6, 7 and 8 show the experimental characteristic curves in terms of T^*, Δp^* and η vs. U^* respectively. It is important to highlight that the torque exerted by the fluid flow on the blades, T_t, is different from the one measured by means of the torque meter, $T_{Torque\ meter}$. Indeed, as stated in equation 7, this is due to the presence of mechanical frictions (mainly on bearings), aerodynamic windage (due to air turbulence and shear on the shaft and the turbine hub) and flywheel effects (here negligible since the test is at constant rotational speed). In order to correctly consider windage and friction losses, the turbine has been tested at different rotation speed in absence of any flow rate. This condition can be performed by simply keeping the wind tunnel blower turned off, $T_{Torque\ meter}^{(v=0m/s)}$. However, under such flow conditions, the torque meter not only measures the windage and friction losses but also the drag effect of the turbine blades, viewing a relative flow at an angle of attack equal to 0 deg, $T_t^{(v=0m/s)}$. This drag effect has been derived from 3D CFD simulation performed in previous works by Torresi et al. [12] [13] [14]. Finally, the aerodynamic turbine torque, T_t, can be derived according to equation 7:

$$T_t = -T_{Torque\ meter} + T_{Torque\ meter}^{(v=0m/s)} - T_t^{(v=0m/s)} \tag{7}$$

From figure 6, it is possible to notice how the torque coefficient, T^*, becomes positive for $U^* > 0.07$. This implies that the Wells turbine under investigation is not self-starting. Indeed, for $U^* < 0.07$ the turbine needs to be driven by the electric motor. For this reason, in figure 7 no efficiency values are reported up to $U^* = 0.07$, whereas the highest efficiency occurs at $U^* = 0.164$, $\eta_{max} = 0.352$. Moreover, the torque coefficient, T^*, increases up to $U^* = 0.19$ then drastically decreases for higher flow coefficients because the turbine works under stall conditions, i.e. the relative air flow is no more able to follow the aerodynamic blade profile and flow separation occurs.

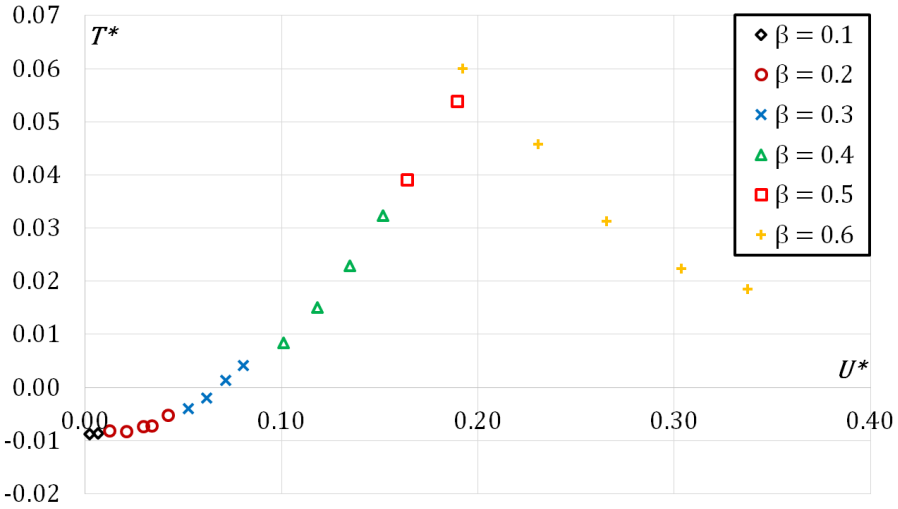

FIGURE 6. Torque coefficient, T^*, vs. flow coefficient, U^*.

Figure 8 shows an important characteristic of this kind of machine, i.e. the linear behavior of the non-dimensional pressure drop, Δp^*, with respect to the flow coefficient, U^*.

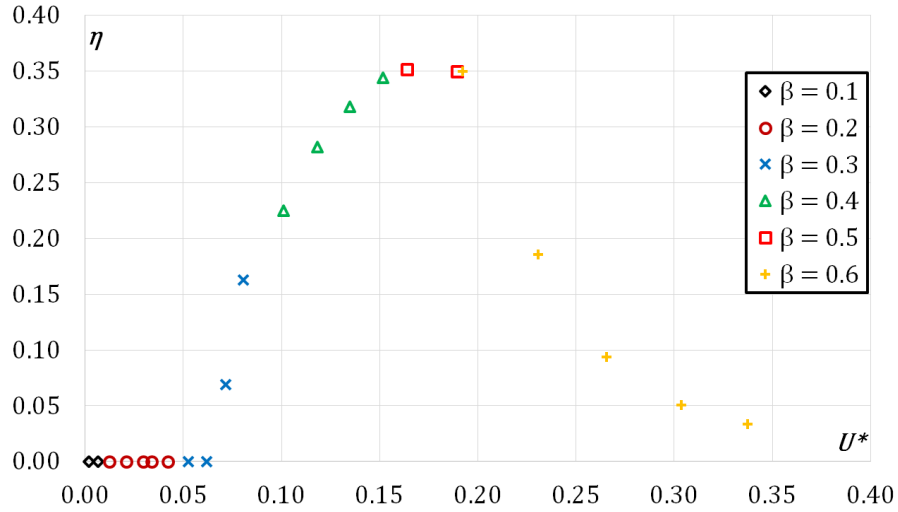

FIGURE 7. Non dimensional pressure drop, Δp^*, vs. flow coefficient, U^*.

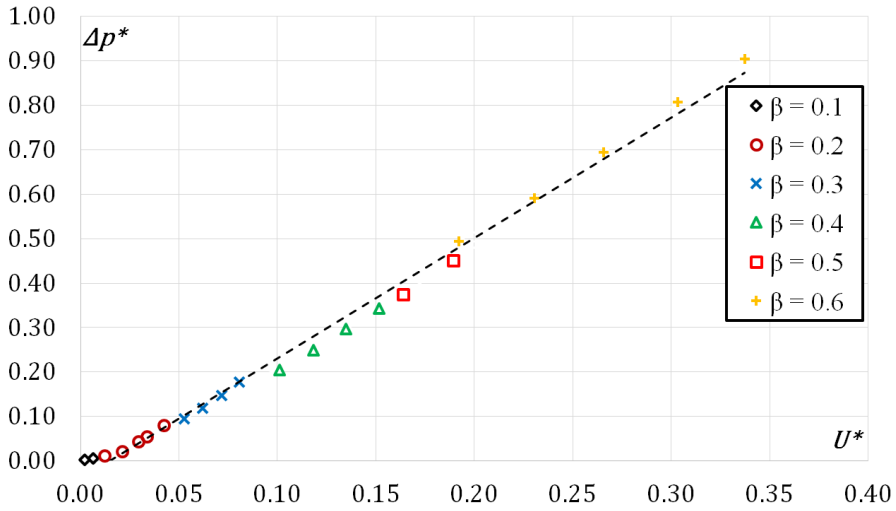

FIGURE 8. Wells turbine efficiency, η, vs. flow coefficient, U^*.

Finally, in order to simulate the actual working condition in an OWC system, the turbine has been tested under unsteady flow conditions. Actually, a pulsating flow rate has been imposed by changing sinusoidally the frequency of the vector control drive, hence the rotational speed of the blower. Figure 9 represents the average mass flow rates, G, and inverter frequency, f, measured during unsteady tests for each data sample, evidencing a delay in the mass flow rate variation. In order to prove this, in Figure 9, a third curve is represented, obtained by considering the mass flow rate values computed at each frequency and then shifting it in order to superpose this curve to the averaged unsteady mass flow rate.

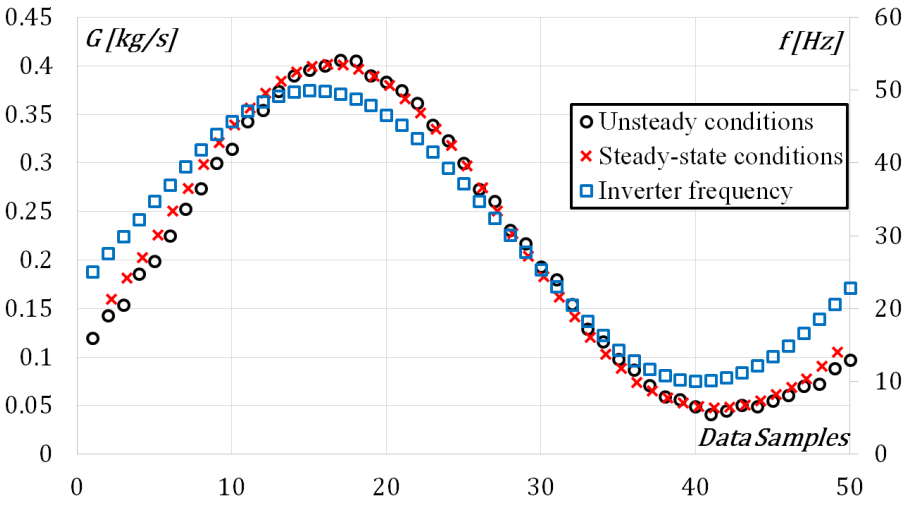

FIGURE 9. Comparison of the mass flow rates during steady and unsteady experimental tests.

Two tests have been performed in order to investigate the unsteady behavior of the turbine in both the normal working condition ($U^* \leq 0.19$) and the stall zone ($U^* > 0.19$). Indeed, figure 10a shows the comparison between the steady state T^*curve at 1750 rpm and the unsteady T^* curve obtained by keeping constant the turbine rotational speed at the same value and varying sinusoidally the frequency of the vector control drive connected to the wind tunnel blower (period, T = 20 s, amplitude, A = 10 Hz and mean value, $\bar{f}$ = 20 Hz). Under this flow condition, there is no hysteresis cycle since the turbine is working in absence of any flow separation. This is coherent with the findings of Ghisu et al., who proved that the hysteresis in Wells turbines is mainly caused by compressibility effects within the

air chamber (i.e. a phase delay between piston speed and turbine mass-flow) and not by an aerodynamic hysteresis of the turbine [15-16].

A different behavior occurs when the turbine experiences large oscillations of the flow coefficient at high mass flow rates, as showed in figure 10b. In this case, the frequency of the vector control drive connected to the wind tunnel blower has been changed with a sinusoidal frequency of period, T = 20 s, amplitude A = 20 Hz and mean value, $\bar{f}$ = 30 Hz. Under this flow condition, a clockwise hysteretic loop appears due to blade dynamic stall,

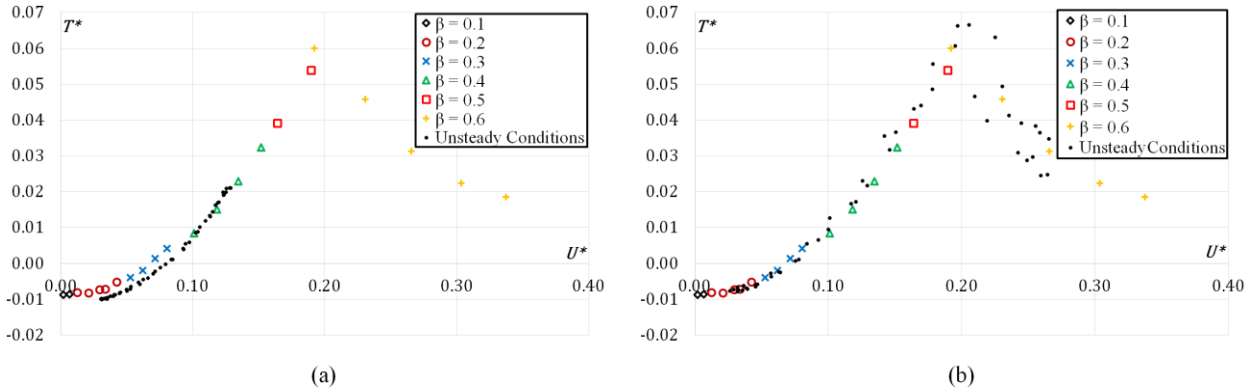

FIGURE 10. Detailed drawing of the small-scale Wells turbine.

CONCLUSIONS

In conclusion, in this work a Wells turbine has been designed and manufactured by means of a 3-D printer. Then the machine has been tested at the GaVe-PrInCE laboratory of the Polytechnic University of Bari in order to investigate its performance both in steady-state and unsteady flow conditions. The experimental performance curves of the machine have been presented in terms of non-dimensional parameters, namely, torque and pressure drop coefficients and efficiency.

During the tests, the Wells turbine was controlled at constant rotational speed, whereas the mass flow rate through the wind tunnel was increased in order to explore the turbine behaviour at different flow coefficients.

From the experimental data, it has been confirmed that the non-dimensional pressure drop curve shows an almost linear behavior with respect to the flow coefficient. This is fundamental in order to correctly couple the Wells turbine with the OWC device.

The unsteady flow conditions have been performed by creating a sinusoidal pulsating flow. In this way, it has been possible to investigate how the hysteresis cycle changes during both the design working conditions and the dynamic stall phenomenon.

ACKNOWLEDGMENTS

The authors gratefully acknowledge Javier Baigorri, Domenico Panunzio and Alfonso Gagliano for their help during the experimental activities.

REFERENCES

1. IRENA, *Global Energy Transformation: A roadmap to 2050* (International Renewable Energy Agency, Abu Dhabi, 2019).
2. M. Torresi and S. M. Camporeale, “Wind tunnel measurements for the characterization of a small scale monoplane Wells turbine” in *Proceedings of the International Workshop on Metrology for the Sea; Learning to Measure Sea Health Parameters*, (IEEE, 2018), pp. 252–256.
3. F. Adamo, G. Andria, O. Bottiglieri, F. Cotecchia, A. Di Nisio, D. Miccoli, F. Sollecito, M. Spadavecchia, F. Todaro, A. Trotta and C. Vitone, Measurement **127**, (2018).

4. G. Mørk, S. Barstow, A. Kabuth and M. Pontes, "Assessing the Global Wave Energy Potential" in *Proceedings of the 29th International Conference on Ocean, Offshore and Arctic Engineering*, 3 (ASME, 2010), pp. 447–454.
5. A. M. Cornett, "A Global Wave Energy Resource Assessment" in *Proceedings of the 18th International Offshore and Polar Engineering Conference*, (2008).
6. I. López, J. Andreu, S. Ceballos, I. Martinez de Alegria and I. Kortabarria, Renewable and Sustainable Energy Reviews **27**, (2013).
7. I. Hashem, H. S. Abdel Hameed and M. H. Mohamed, Ocean Engineering **164**, (2018).
8. S. Raghunathan, Prog. Aerospace Sci. **31**, (1995).
9. T. Ghisu, P. Puddu and F. Cambuli, Journal of Thermal Science **24**, (2015).
10. M. Torresi, S. M. Camporeale and G. Pascazio, Journal of Fluids Engineering **131 (7)**, (2009).
11. J. C. C. Henriques and L. M. C. Gato, Computational Mechanics **29**, (2002).
12. M. Torresi, S. M. Camporeale and G. Pascazio, "Performance of a small prototype of a high solidity wells turbine" in *Proceedings of the 7th European Conference on Turbomachinery: Fluid Dynamics and Thermodynamics* (ETC, 2007).
13. M. Torresi, S. M. Camporeale and G. Pascazio, "Experimental and numerical investigation on the performance of a Wells turbine prototype" in *Proceedings of the 7th European Wave and Tidal Energy Conference* (2007).
14. M. Torresi, S. M. Camporeale and G. Pascazio, Renewable Energy **33**, (2008)
15. T. Ghisu, P. Puddu, F. Cambuli and I. Virdis, "On the Hysteretic Behaviour of Wells Turbines" in *Proceedings of the 72nd Conference of the Italian Thermal Machines Engineering Association*, Energy Procedia 126 (Elsevier, 2017), pp. 706–713.
16. I. Virdis, T. Ghisu, F. Cambuli and P. Puddu, "A Lumped Parameter Model for the Analysis of Dynamic Effects in Wells Turbines" in *Proceedings of the 73rd Conference of the Italian Thermal Machines Engineering Association*, Energy Procedia 148 (Elsevier, 2018), pp. 503–510.